Available online at www.sciencedirect.com
SCIENCE DIRECT®
Journal of Sound and Vibration 272 (2004) 1047–1069
JOURNAL OF SOUND AND VIBRATION
www.elsevier.com/locate/jsvi

A preliminary investigation into optimising the response of vibrating systems used for ultrasonic cutting

F.C.N. Lim, M.P. Cartmell*, A. Cardoni, M. Lucas

Department of Mechanical Engineering, University of Glasgow, James Watt Building, Glasgow G12 8QQ, UK

Received 2 January 2003; accepted 24 March 2003

Abstract

The coupling of two non-linear oscillators is investigated, each with opposing non-linear overhang characteristics in the frequency domain as a result of positive and negative cubic stiffness. This leads to the definition of a two-degree-of-freedom Duffing oscillator in which such non-linear effects can be neutralised under certain dynamic conditions. The physical motivation for this system stems from applications in ultrasonic cutting in which an exciter drives a tuned blade. The exciter and the blade are both strongly non-linear, with features strongly reminiscent of positive and negative cubic effects. It is shown by means of approximate analysis that in the case of simple idealised coupled oscillator models a practically useful mitigating effect on the overall non-linear response of the system is observed when one of the cubic stiffnesses is varied. Experimentally, it has also been demonstrated that coupling of ultrasonic components with different non-linear characteristics can strongly influence the performance of the system and that the general behaviour of the hypothetical theoretical model is indeed borne out in practice.

1. Introduction

Mechanical and structural systems are inherently non-linear with many sources of non-linearities present in any practical system under consideration. Non-linearities necessarily introduce a whole range of phenomena that are not found in linear systems, including the well-known jump phenomenon, occurrence of multiple solutions, modulations, shifts in natural frequencies, the generation of combination resonances, evidence of period-multiplying bifurcations, and chaotic motions [1–3].

*Corresponding author. Tel.: +44-0141-330-4337; fax: +44-0141-330-4343.
E-mail address: matthewc@mech.gla.ac.uk (M.P. Cartmell).

0022-460X/$ - see front matter © 2003 Elsevier Ltd. All rights reserved.
doi:10.1016/j.jsv.2003.03.011

Material and constitutive non-linearities are frequently encountered in vibration isolators in which polymeric materials are extensively used to reduce the deleterious effects of unwanted vibration. Non-linearities in these system can also arise from geometrical effects, the mode of loading, or various combined phenomena involving material properties, geometrical configuration, and loading characteristics. Softening effects due to material properties have been identified and published [4–6], and these findings have specifically centred around polymeric materials in terms of their stiffness and damping characteristics.

Many studies have been dedicated to the Duffing oscillator in different attempts to quantify and map the local and global dynamics of systems in which softening and hardening non-linearities feature significantly. An early article by Morozov [7] presented a qualitative study of a softening Duffing equation, viz., the boundedness of the number of resonances and periodic solutions, the existence of heteroclinic solutions and the behaviour of solutions in a neighbourhood of an unperturbed separatrix contour. In the early 1980s, Ueda [8,9] extensively studied the steady state chaotic behaviour, and randomly transitional phenomena, in a system governed by a hardening Duffing equation. He has shown that the non-linear system under consideration can exhibit chaotic responses (under harmonic excitation) in certain parameter regimes. By combining second order perturbation solutions and assessment of stability by means of Floquet analysis, Nayfeh and Sanchez [3] developed an approximate procedure for the generation of bifurcation diagrams in a forced softening Duffing oscillator. In a non-linear system, jump phenomena occur regularly and a hardening system reported by Soliman [10] showed that for small excitation levels the system exhibits what appears to be linear behaviour, however this invariably becomes non-linear as the excitation levels are increased, and unpredictable jumps *to* and *from* resonance are clearly evident.

The application of high power ultrasonic tooling to manufacturing processes is a well-established area of research and one which has shown great potential. However, ultrasonic machining and cutting processes have been rather under-exploited in industry due to reliability problems associated with the non-linear behaviour of the various components that are used. Design strategies such as ensuring vibrational uniformity and acceptable stresses in the block horns, or blades, really have to be implemented for reliable tuned ultrasonic systems [11–14]. However, by investigating and modelling the influence of ultrasonic energy generation and its interaction with the beneficial mechanisms in ultrasonic tooling, other solutions related to the measured non-linear coupling effects can be formulated. The state of the art is not by any means entirely clear-cut and so reliability limitations imposed by deficiencies in current design practices are treated in this paper by a new attempt to exploit a mechanistic understanding of ultrasonic system non-linearities. The outcome is a reliable tuned ultrasonic tool design strategy which is potentially adaptable to a wide range of manufacturing processes.

Recently, research on the response of systems exhibiting non-linear cubic damping has been reported by Shekhar et al. [15] who studied the effect of non-linear damping on the performance of a single-degree-of-freedom shock isolator system and showed that this appreciably affects the response. Specifically, a small negative coefficient for the damping term is more favourable than a positive coefficient in generating a considerable reduction in the peak of the acceleration response. In a follow-up paper, the same authors [16] proposed that three-element and two-stage isolators are more effective when in the presence of non-linear cubic damping. In another publication, Ravindra and Mallik [17] showed how non-linear damping could be used as a passive mechanism to suppress chaos.

In the well-known publication by Ott et al. [18], chaos is controlled by careful choice of a small perturbation parameter in order to create a variety of attracting periodic motions, from which the most desirable attractor can be selected. Since this postulation was made, interest in such approaches has increased, and has been applied in a variety of physical experiments [19–24].

High frequency parametric vibration and amplitude modulation of the forcing function have both been used by Chow and Maestrello [24] as the basis for a general method of vibrational control for a certain class of non-linear evolution equations. The use of high frequency parametric vibration introduces a change in some system parameter in order to ensure static stability, whilst forcing amplitude modulation, if needed, can be used to stabilise an unstable periodic motion. Maestrello [25] used a method that requires knowledge of the initial unstable disturbances in terms of frequency, amplitude and phase, or their equivalent temporal values, to cancel growth after several bifurcations from periodic to chaotic states.

In this paper, preliminary investigations into vibration response modifications in coupled oscillators are discussed. In order to establish a systematic basis for this, a simple coupled oscillator problem is proposed in which two single-degree-of-freedom sub-systems are implemented, with the principal non-linearity being a hardening and softening cubic stiffness effect, respectively, in each. This hypothesised theoretical vehicle in fact closely reflects the characteristics which emerge from measurements made on actual ultrasonic cutting tooling in which serially coupled components are encountered. Such systems routinely exhibit alternate hardening and softening effects in this manner, notwithstanding their more complicated structural form. In the case of the hypothesised theoretical model, the method of multiple scales is used for the perturbation analysis of this two-degree-of-freedom coupled Duffing oscillator. Theoretical results show that controlled variations in the softening stiffness can have a significant effect on the overall non-linear response of the system, thereby making the overall effect hardening, softening, or approximately linear. So, although this model is not intended to define literally a typical ultrasonic cutting system it is still of use in that it consolidates a major phenomenon which is readily observable in such systems, and on that basis has intrinsic value.

The experimental ultrasonic system is not directly modelled in this paper, however the hypothesised theoretical vehicle is shown to respond in a manner which mirrors that of a typical food industry ultrasonic cutting system. Specifically, serially coupled structural components with different non-linearities (i.e., hardening or softening) are shown to work together in response-modifying ways that are closely predicted by the simplified theoretical model. The fundamentally non-linear component in an ultrasonic cutting system is invariably the ultrasonic exciter (popularly, but incorrectly, known as the *transducer*), in which the effect is mainly attributable to the piezoelectric ceramics. This effect is a predominantly softening cubic stiffness phenomenon [26]. The inter-coupling components between the transducer and the actual blade usually take the form of aluminium or steel bar-horns or block-horns, these being solid, tuned, components with screw-thread connections at each end. The net effect of the bar- or block-horn, together with its screwed connections is a hardening cubic effect. Therefore, in modal terms, the serial combination of an ultrasonic transducer driving a tuned bar- or block-horn is that of a pair of single-degree-of-freedom sub-systems (in the modal domain) in which softening and hardening characteristics can mutually mitigate in order to produce broadly linear responses at the cutting blade.

The non-linear cubic effects in the hypothesised theoretical model manifest as controllable design variables in the experimental system. Principally these comprise transducer output level

(nominally controlled by voltage and temperature) and the physical form of the bar or block horn, the tightening torque applied to the screwed joints, and also the actual position of the screw stud inside the joints.

This paper explores the behaviour of the hypothesised theoretical model and then attempts to show that judicious attention to the same class of principal non-linearities in the experimental system can lead to improved designs for practical ultrasonic cutting systems.

2. Hypothesised theoretical model

The theoretical model of this system takes the convenient simplified form of a two-degree-of-freedom Duffing oscillator system, as shown in Fig. 1. The model is taken to have linear damping, as defined by coefficients c_1, and c_2, and linear stiffnesses, together with attendant non-linear cubic stiffnesses, k_1, k_2 and h_1, h_2, respectively. The non-linear stiffness quantity h_1 comprises a hardening spring defined by $+h_1x_1^{*3}$ and h_2 constitutes a softening spring defined by $-h_2x_2^{*3}$. A harmonic excitation force $F_1^*(t) = F^*\cos\Omega^* t^*$ is applied to the first sub-system.

2.1. Equations of motion

The governing differential equations of the system are directly derived via Lagrange's equations and emerge in the form of,

$$m_1\ddot{x}_1^* + c_1\dot{x}_1^* + c_2(\dot{x}_1^* - \dot{x}_2^*) + k_1x_1^* + k_2(x_1^* - x_2^*) + h_1(x_1^*)^3 + h_2(x_2^* - x_1^*)^3 = F^*\cos\Omega^* t^*, \quad (1)$$

$$m_2\ddot{x}_2^* + c_2(\dot{x}_2^* - \dot{x}_1^*) + k_2(x_2^* - x_1^*) - h_2(x_2^* - x_1^*)^3 = 0, \quad (2)$$

where $x_{1,2}^* = x_{1,2}^*(t^*)$ and the star represents variables which still, at this stage, possess physical dimensions.

By introducing dimensionless time $t = \omega_{e1}t^*$, where

$$\omega_{e1} = \sqrt{\frac{1}{2}\left[\frac{k_1}{m_1} + \frac{k_2}{m_1} + \frac{k_2}{m_2} - \sqrt{\left(\frac{k_1}{m_1}\right)^2 + \frac{2k_1}{m_1}\left(\frac{k_2}{m_1} - \frac{k_2}{m_2}\right) + \left(\frac{k_2}{m_1} + \frac{k_2}{m_2}\right)^2}\right]} \quad (3)$$

is the undamped linear natural frequency, then non-dimensional response co-ordinates in the form of $x_{1,2} = x_{1,2}^*/x_{ref}^*$, where x_{ref}^* can be an arbitary reference displacement are introduced.

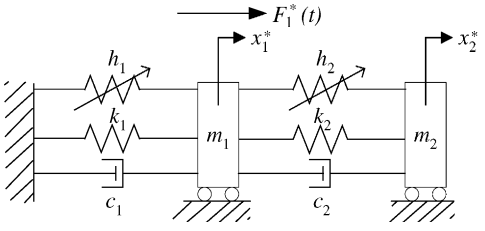

Fig. 1. Schematic representation of the hypothesised model.

Therefore, in terms of dimensionless time, one rewrites Eqs. (1) and (2) as

$$x_1'' + 2\varepsilon\tilde{\zeta}_1 x_1' + 2\varepsilon\tilde{\zeta}_2(x_1' - x_2') + \gamma_1 x_1 + \varepsilon\tilde{\gamma}_2(x_1 - x_2) + \varepsilon\tilde{\eta}_1(x_1)^3 + \varepsilon\tilde{\eta}_2(x_2 - x_1)^3 = \varepsilon\tilde{F}\cos\Omega t, \quad (4)$$

$$x_2'' + 2\varepsilon\tilde{\zeta}_3(x_2' - x_1') + \gamma_3(x_2 - x_1) - \varepsilon\tilde{\eta}_3(x_2 - x_1)^3 = 0, \quad (5)$$

where $x_{1,2} = x_{1,2}(t)$ and

$$\tilde{\zeta}_1 = \frac{c_1}{2\varepsilon m_1\omega_{e1}}; \quad \tilde{\zeta}_2 = \frac{c_2}{2\varepsilon m_1\omega_{e1}}; \quad \tilde{\zeta}_3 = \frac{c_2}{2\varepsilon m_2\omega_{e1}}; \quad \gamma_1 = \frac{k_1}{m_1\omega_{e1}^2}; \quad \tilde{\gamma}_2 = \frac{k_2}{\varepsilon m_1\omega_{e1}^2}; \quad \gamma_3 = \frac{k_2}{m_2\omega_{e1}^2};$$
$$\tilde{\eta}_1 = \frac{h_1 x_{ref}^{*2}}{\varepsilon m_1\omega_{e1}^2}; \quad \tilde{\eta}_2 = \frac{h_2 x_{ref}^{*2}}{\varepsilon m_1\omega_{e1}^2}; \quad \tilde{\eta}_3 = \frac{h_2 x_{ref}^{*2}}{\varepsilon m_2\omega_{e1}^2}; \quad \tilde{F} = \frac{F^*}{\varepsilon m_1\omega_{e1}^2 x_{ref}^*}; \quad \Omega = \frac{\Omega^*}{\omega_{e1}}. \quad (6)$$

Motions in the neighbourhood of the static equilibrium position are considered so that the amplitude of the response is assumed to be of the order of some small parameter ε, $0 < \varepsilon \ll 1$. All the terms in Eqs. (4) and (5) are re-formulated in terms of this small parameter, ε, with the exception of the linear inertia terms, and the linear stiffness terms containing γ_1 and γ_3. This ensures that all other effects only appear within the higher order perturbation equations, whereas the aforementioned terms appear in the zeroth order perturbation equations from which the necessary generating solutions are obtained [27].

2.2. Perturbation solution of the equations of motion

The classical method of multiple scales [28–31] has been used to solve the equations up to and including first order perturbation. The co-ordinates $x_{1,2}$, and the first and second total derivatives, are stated in power series form, in the usual way,

$$x_1 = x_{10} + \varepsilon x_{11} + \varepsilon^2 x_{12} + \cdots + \varepsilon^n x_{1n}, \quad x_2 = x_{20} + \varepsilon x_{21} + \varepsilon^2 x_{22} + \cdots + \varepsilon^n x_{2n}, \quad (7,8)$$

$$\frac{\mathrm{d}}{\mathrm{d}t} = \mathrm{D}_0 + \varepsilon\mathrm{D}_1 + \varepsilon^2\mathrm{D}_2 + \cdots + \varepsilon^n\mathrm{D}_n, \quad \frac{\mathrm{d}}{\mathrm{d}t^2} = \mathrm{D}_0^2 + 2\varepsilon\mathrm{D}_0\mathrm{D}_1 + \cdots, \quad (9,10)$$

where x_{1n} and x_{2n} in Eqs. (7) and (8) represent functions of timescales T_n (i.e., $T_0 = t$ and $T_1 = \varepsilon t$). The partial derivatives of Eqs. (9) and (10) are stated in the standard D operator notation where $\mathrm{D}_i^j = \partial^j/\partial T_i^j$. Series (7)–(10), inclusive, are truncated after the first order ε terms because this perturbation analysis is limited to first order level.

Applying the method of multiple scales in the conventional manner, Eqs. (7)–(10) are substituted into Eqs. (4) and (5), and then coefficients of like order of ε are grouped together to lead to:

Order ε^0:

$$\mathrm{D}_0^2 x_{10} + \omega_1^2 x_{10} = 0, \quad \mathrm{D}_0^2 x_{20} + \omega_2^2 x_{20} - \omega_2^2 x_{10} = 0. \quad (11,12)$$

Order ε:

$$\mathrm{D}_0^2 x_{11} + \omega_1^2 x_{11} = \tilde{F}\cos\Omega t - 2\mathrm{D}_0\mathrm{D}_1 x_{10} - 2\tilde{\zeta}_1\mathrm{D}_0 x_{10} - 2\tilde{\zeta}_2\mathrm{D}_0 x_{10} + 2\tilde{\zeta}_2\mathrm{D}_0 x_{20} - \tilde{\gamma}_2 x_{10} + \tilde{\gamma}_2 x_{20}$$
$$- \tilde{\eta}_1 x_{10}^3 - \tilde{\eta}_2(x_{20}^3 + 3x_{10}^2 x_{20} - 3x_{10}x_{20}^2 - x_{10}^3), \quad (13)$$

$$\mathrm{D}_0^2 x_{21} + \omega_2^2 x_{21} = 2\tilde{\zeta}_3 \mathrm{D}_0 x_{10} - 2\mathrm{D}_0\mathrm{D}_1 x_{20} - 2\tilde{\zeta}_3 \mathrm{D}_0 x_{20} + \omega_2^2 x_{11} + \tilde{\eta}_3 (x_{20}^3 + 3x_{10}^2 x_{20} - 3x_{10} x_{20}^2 - x_{10}^3), \tag{14}$$

where

$$\omega_1^2 = \gamma_1, \quad \omega_2^2 = \gamma_3. \tag{15, 16}$$

Harmonic solutions to Eqs. (11) and (12) can be expressed in convenient polar form as

$$x_{10} = A_1(T_1)\,\mathrm{e}^{\mathrm{i}\omega_1 T_0} + \bar{A}_1(T_1)\,\mathrm{e}^{-\mathrm{i}\omega_1 T_0}, \tag{17}$$

$$x_{20} = A_2(T_1)\,\mathrm{e}^{\mathrm{i}\omega_2 T_0} + \bar{A}_2(T_1)\,\mathrm{e}^{-\mathrm{i}\omega_2 T_0} + A_3(T_1)\,\mathrm{e}^{\mathrm{i}\omega_1 T_0} + \bar{A}_3(T_1)\,\mathrm{e}^{-\mathrm{i}\omega_1 T_0}, \tag{18}$$

where $A_3 = \Gamma A_1 = (\omega_2^2/(\omega_2^2 - \omega_1^2))A_1$, the overbar denotes complex conjugacy, and $\mathrm{i} = \sqrt{-1}$.

The functions $A_{1,2,3}$ are arbitrary at this level of approximation but are determined by elimination of the secular terms from the next order of perturbation.

The behaviour of this relatively simple system accommodates the fact that the forcing frequency and natural frequencies can satisfy certain, fundamentally important, external and internal resonance conditions. Since the primary system is excited at Ω, and this can be synchronous with ω_1, or nearly so, then the external resonance condition is given by,

$$\Omega = \omega_1 + \varepsilon v. \tag{19}$$

In addition to this, the analysis shows that the case of superharmonic internal resonance is also feasible,

$$\omega_2 \approx \tfrac{1}{3}\omega_1. \tag{20}$$

This can be expressed, and therefore subsequently explored, by introducing a detuning parameter $\varepsilon\sigma_1$ such that

$$\omega_2 = \tfrac{1}{3}\omega_1 + \varepsilon\sigma_1. \tag{21}$$

The detuning parameters, εv and $\varepsilon\sigma_1$, are conveniently termed *external* and *internal* detuning parameters, respectively. Other internal resonance conditions are also predicted by the analysis, i.e., $\omega_2 = \omega_1$ (primary) and $\omega_2 = 3\omega_1$ (subharmonic), however these do not address the physical phenomenon under investigation and are therefore not discussed further.

Substituting Eqs. (17) and (18) into Eq. (13), and then extracting the terms that produce secular terms in x_{11} for superharmonic resonance yields the following solvability condition for the first order expansion, noting that the general approach of multiple scales is to equate the secular terms in Eqs. (22) and (24) to zero so as to preserve the uniformity of the expansion,

$$\begin{aligned}&\tfrac{1}{2}\mathrm{e}^{\mathrm{i}\varepsilon v T_0}\tilde{F} - \mathrm{e}^{\mathrm{i}\varepsilon 3\sigma_1 T_0}\tilde{\eta}_2 A_2^3 - \tilde{\gamma}_2 A_1 - \mathrm{i}2\omega_1\tilde{\zeta}_1 A_1 - \mathrm{i}2\omega_1\tilde{\zeta}_2 A_1 - 3\tilde{\eta}_1 A_1^2\bar{A}_1 + 3\tilde{\eta}_2 A_1^2\bar{A}_1 - 3\tilde{\eta}_2 A_1^2\bar{A}_3 \\ &\quad + 6\tilde{\eta}_2 A_1 A_2\bar{A}_2 + \tilde{\gamma}_2 A_3 + \mathrm{i}2\omega_1\tilde{\zeta}_2 A_3 - 6\tilde{\eta}_2 A_1 A_3\bar{A}_1 + 6\tilde{\eta}_2 A_1 A_3\bar{A}_3 - 6\tilde{\eta}_2 A_2 A_3\bar{A}_2 + 3\tilde{\eta}_2 A_3^2\bar{A}_1 \\ &\quad - 3\tilde{\eta}_2 A_3^2\bar{A}_3 - \mathrm{i}2\omega_1 A_1' + \text{c.c.} = 0,\end{aligned} \tag{22}$$

where the prime indicates differentiation with respect to T_1 and c.c. represents the complex conjugates of the preceding terms. The uniform solution of Eq. (13) can now be written as

$$x_{11} = e^{i\omega_2 T_0}\left(\frac{1}{\omega_1^2-\omega_2^2}\left(\tilde{\gamma}_2 A_2 + i2\omega_2\tilde{\zeta}_2 A_2 - 6\tilde{\eta}_2 A_1 A_2 \bar{A}_1 + 6\tilde{\eta}_2 A_1 A_2 \bar{A}_3 - 3\tilde{\eta}_2 A_2^2 \bar{A}_2 + 6\tilde{\eta}_2 A_2 A_3 \bar{A}_1 - 6\tilde{\eta}_2 A_2 A_3 \bar{A}_3\right)\right) + \text{terms proportional to } e^{i(2\omega_2+\omega_1)T_0}, e^{i3\omega_1 T_0}, e^{i(\omega_2-2\omega_1)T_0}, e^{i(\omega_2+2\omega_1)T_0}, e^{i(2\omega_2-\omega_1)T_0} + \text{c.c.} \quad (23)$$

Substituting Eq. (23) into Eq. (14), because of the explicit presence of $\omega_2^2 x_{11}$ in the right hand side of Eq. (14), and then identifying the secular terms for x_{21} results in,

$$e^{i(\omega_1-3\omega_2)T_0}\left(-3\tilde{\eta}_3 A_1 \bar{A}_2^2 + 3\tilde{\eta}_3 A_3 \bar{A}_2^2 + \left(3\omega_2^2\tilde{\eta}_2 A_1 \bar{A}_2^2/4\omega_1\omega_2 - 4\omega_2^2\right) - \left(3\omega_2^2\tilde{\eta}_2 A_3 \bar{A}_2^2/4\omega_1\omega_2 - 4\omega_2^2\right)\right) + \Gamma\left(\tilde{\gamma}_2 A_2 + i2\omega_2\tilde{\zeta}_2 A_2 - 6\tilde{\eta}_2 A_1 A_2 \bar{A}_1 + 6\tilde{\eta}_2 A_1 A_2 \bar{A}_3 - 3\tilde{\eta}_2 A_2^2 \bar{A}_2 + 6\tilde{\eta}_2 A_2 A_3 \bar{A}_1 - 6\tilde{\eta}_2 A_2 A_3 \bar{A}_3\right) - i2\omega_2\tilde{\zeta}_3 A_2 + 6\tilde{\eta}_3 A_1 A_2 \bar{A}_1 - 6\tilde{\eta}_3 A_1 A_2 \bar{A}_3 + 3\tilde{\eta}_3 A_2^2 \bar{A}_2 - 6\tilde{\eta}_3 A_2 A_3 \bar{A}_1 + 6\tilde{\eta}_3 A_2 A_3 \bar{A}_3 - i2\omega_2 A_2' + \text{c.c.} = 0. \quad (24)$$

The complex amplitudes A_1 and A_2 can then be expressed in polar forms as

$$A_n = \tfrac{1}{2} a_n e^{i\beta_n[T_1]}, \quad \bar{A}_n = \tfrac{1}{2} a_n e^{-i\beta_n[T_1]}, \quad (25)$$

where a_n and β_n are real. From this position the real and imaginary terms can then be separated out to generate four modulation equations,

$$(\tilde{F}/2)\cos\Lambda_1 - \tfrac{1}{2}\tilde{\gamma}_2 a_1 + \tfrac{1}{2}\Gamma\tilde{\gamma}_2 a_1 + (-\tfrac{3}{8}\tilde{\eta}_1 + \tfrac{3}{8}\tilde{\eta}_2 - \tfrac{9}{8}\Gamma\tilde{\eta}_2 + \tfrac{9}{8}\Gamma^2\tilde{\eta}_2 - \tfrac{3}{8}\Gamma^3\tilde{\eta}_2)a_1^3 + \tfrac{3}{4}\tilde{\eta}_2 a_1 a_2^2 - \tfrac{3}{4}\Gamma\tilde{\eta}_2 a_1 a_2^2 - \tfrac{1}{8}\cos\Phi_1\tilde{\eta}_2 a_2^3 + \omega_1 a_1\beta_1' = 0, \quad (26)$$

$$(F/2)\sin\Lambda_1 - \omega_1\tilde{\zeta}_1 a_1 - \omega_1\tilde{\zeta}_2 a_1 + \Gamma\omega_1\tilde{\zeta}_2 a_1 - \tfrac{1}{8}\sin\Phi_1\tilde{\eta}_2 a_2^3 - \omega_1 a_2' = 0, \quad (27)$$

$$\frac{1}{2\omega_1^2-2\omega_2^2}\left(\omega_2^2\tilde{\gamma}_2 a_2 + 3\Gamma\omega_2^2\tilde{\eta}_2 a_1^2 a_2\right) - \frac{1}{4\omega_1^2-4\omega_2^2}\left(3\omega_2^2\tilde{\eta}_2 a_1^2 a_2 + 3\Gamma^2\omega_2^2\tilde{\eta}_2 a_1^2 a_2\right) + \frac{1}{32\omega_1\omega_2-32\omega_2^2}\left(3\cos\Phi_1\omega_2^2\tilde{\eta}_2 a_1 a_2^2 - 3\Gamma\cos\Phi_1\omega_2^2\tilde{\eta}_2 a_1 a_2^2\right) - \frac{3\omega_2^2\tilde{\eta}_2 a_2^3}{8\omega_1^2-8\omega_2^2} + \left(\tfrac{3}{4}\tilde{\eta}_3 - \tfrac{3}{2}\Gamma\tilde{\eta}_3 + \tfrac{3}{4}\Gamma^2\tilde{\eta}_3 + \tfrac{3}{8}\cos\Phi_1\tilde{\eta}_3 + \tfrac{3}{8}\Gamma\cos\Phi_1\tilde{\eta}_3\right)a_1^2 a_2 + \tfrac{3}{8}\tilde{\eta}_3 a_2^3 + \omega_2 a_2\beta_2' = 0, \quad (28)$$

$$\frac{\omega_2^3\tilde{\zeta}_2 a_2}{\omega_1^2-\omega_2^2} + \frac{3\sin\Phi_1\omega_2^2\tilde{\eta}_2 a_1 a_2^2}{32\omega_1\omega_2-32\omega_2^2}(\Gamma-1) + \tfrac{3}{8}\sin\Phi_1\tilde{\eta}_3 a_1 a_2^2(1-\Gamma) - \omega_2\tilde{\zeta}_3 a_2 - \omega_2 a_2' = 0, \quad (29)$$

where

$$\Lambda_1 = \nu_1 T_1 - \beta_1, \quad \Phi_1 = 3\sigma_1 T_1 - \beta_1 + 3\beta_2. \quad (30, 31)$$

The form of Eqs. (26)–(29) renders the system autonomous. If the following conditions are used to impose steady state conditions,

$$a_1' = a_2' = \Lambda_1' = \Phi_1' = 0 \tag{32}$$

and then Eqs. (30) and (31) are differentiated with respect to T_1 leading to

$$\beta_1' = \nu_1, \quad \beta_2' = \tfrac{1}{3}\nu_1 - \sigma_1 \tag{33, 34}$$

then substitution of Eqs. (32)–(34) into Eqs. (26)–(29) will lead to two approximate analytical forms from which the amplitudes of the system can be obtained when it is undergoing the synchronous external resonance of Eq. (19) and the superharmonic internal resonance defined in Eq. (21). The presence of ε in Eqs. (35) and (36) allows a return to the original physically defined parameters, thus,

$$\begin{aligned}
&1296\varepsilon\tilde{F}^2\left((\Gamma-1)^2(\omega_1+\omega_2)^2(\omega_2\varepsilon\tilde{\eta}_2+4(\omega_2-\omega_1)\varepsilon\tilde{\eta}_3)^2a_1^2\right)\\
&\quad=\left(\omega_1\left(\varepsilon\tilde{\zeta}_1-(\Gamma-1)\varepsilon\tilde{\zeta}_2\right)a_1-\frac{4\omega_2(\omega_2^2(\varepsilon\tilde{\zeta}_2+\varepsilon\tilde{\zeta}_3)-\omega_1^2\varepsilon\tilde{\zeta}_3)\varepsilon\tilde{\eta}_2a_2^2}{3(\Gamma-1)(\omega_1+\omega_2)(\omega_2\varepsilon\tilde{\eta}_2+4(\omega_2-\omega_1)\varepsilon\tilde{\eta}_3)a_1}\right)^2\\
&\qquad+\left(\begin{array}{c}9(\Gamma-1)(\omega_1+\omega_2)(4\omega_1\varepsilon\tilde{\eta}_3-\omega_2(\varepsilon\tilde{\eta}_2+4\varepsilon\tilde{\eta}_3))a_1^2(8\varepsilon\nu_1\omega_1+4(\Gamma-1)\varepsilon\tilde{\gamma}_2\\ -3(\varepsilon\tilde{\eta}_1+(\Gamma-1)^3\varepsilon\tilde{\eta}_2)a_1^2)+2\varepsilon\tilde{\eta}_2(8\omega_2(2(\varepsilon\nu_1-3\varepsilon\sigma_1)(\omega_1^2-\omega_2^2)+3\omega_2\varepsilon\tilde{\gamma}_2)\\ -9(\Gamma-1)^2(\omega_2(\omega_2-3\omega_1)\varepsilon\tilde{\eta}_2+8(\omega_1^2-\omega_2^2)\varepsilon\tilde{\eta}_3)a_1^2)a_2^2\\ -36\varepsilon\tilde{\eta}_2(\omega_2^2(\varepsilon\tilde{\eta}_2+\varepsilon\tilde{\eta}_3)-\omega_1^2\varepsilon\tilde{\eta}_3)a_2^4\end{array}\right)^2,
\end{aligned} \tag{35}$$

$$\begin{aligned}
&(\omega_1-\omega_2)^2\left(576\omega_2^2\left(\frac{\omega_2^2\varepsilon\tilde{\zeta}_2}{\omega_2^2-\omega_1^2}+\varepsilon\tilde{\zeta}_3\right)^2+\frac{1}{(\omega_1^2-\omega_2^2)^2}\left(\begin{array}{c}4\omega_2(2(\varepsilon\nu_1-3\varepsilon\sigma_1)(\omega_2^2-\omega_1^2)-3\omega_2\varepsilon\tilde{\gamma}_2)\\ +9(\omega_2^2(\varepsilon\tilde{\eta}_2+\varepsilon\tilde{\eta}_3)-\omega_1^2\varepsilon\tilde{\eta}_3)(2(\Gamma-1)^2a_1^2+a_2^2)\end{array}\right)^2\right).\\
&\quad=\tfrac{81}{16}(\Gamma-1)^2(\omega_2\varepsilon\tilde{\eta}_2+4(\omega_2-\omega_1)\varepsilon\tilde{\eta}_3)^2a_1^2a_2^2.
\end{aligned} \tag{36}$$

Using the expressions in Eqs. (35) and (36), the next section presents some numerical results obtainable for the amplitudes a_1 and a_2, for the superharmonic resonance condition under various conditions.

3. Results

3.1. Approximate analytical responses in the frequency domain

Fig. 2 shows the non-dimensionalised response plots of amplitudes a_1 and a_2 for the case of the superharmonic resonance of Eq. (21). In these plots, the hardening cubic stiffness coefficient h_1, the excitation level, and all system quantities other than the softening cubic stiffness coefficient h_2, are kept constant. It is evident that as h_2 is increased or decreased it affects the general characteristic behaviour of the system. The effect of increasing h_2 manifests as more accentuated softening behaviour (by bending towards the left) in the response of both a_1 and a_2, and

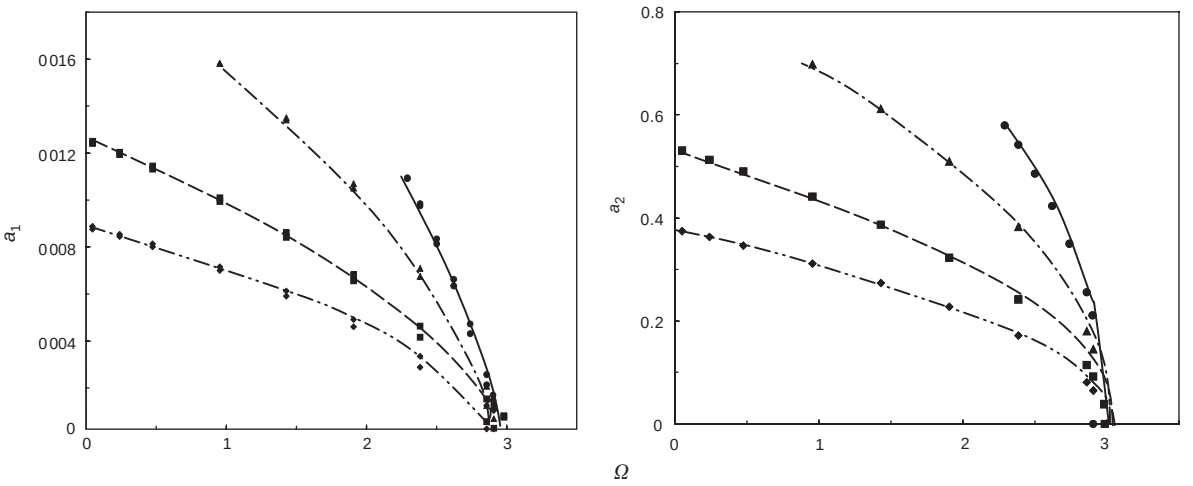

Fig. 2. Non-dimensionalised response plots of the hypothesised theoretical model with $\varepsilon\tilde{\zeta}_1 = \varepsilon\tilde{\zeta}_2 = 5.96 \times 10^{-5}$, $\varepsilon\tilde{\zeta}_3 = 1.06 \times 10^{-4}$, $\varepsilon\tilde{\gamma}_2 = 0.60$, $\varepsilon\tilde{\eta}_1 = 136.28$, $\varepsilon\tilde{F} = 1.14 \times 10^{-3}$, $\varepsilon\sigma_1 = 0$. Key for h_2 values (multiple of h_1): –· ◆ –· ·, 0.083; – – ■ – –, 0.042; –· –▲ –· –, 0.0167; —●—, 0.008.

conversely, a decrease in h_2 will cause the system to be less softening and bend towards a linear response. The most desirable response is when $h_2 = 0.008\,h_1$ for which both responses a_1 and a_2 are more linear in appearance.

3.2. Direct numerical integration

In order to provide another theoretical basis for the comparison with the results from the multiple scales analysis, results from direct numerical integration of the differential equations are presented next. Figs. 3 and 4 show the results of using *NDSolve* in *Mathematica* [32] to numerically integrate Eqs. (1) and (2). Figs. 3a and 4a show the non-dimensionalised logarithmic plot of the amplitude responses x_1 and x_2 with respect to the excitation frequency Ω. The same variables are again kept constant as in Section 3.1, and only the softening cubic stiffness, h_2 is varied.

An upward and downward sweep of the excitation frequency has been carried out for each iteration. The thicker lines denote the upward sweeps while the thinner lines denote the downward sweeps. It is clearly seen from Figs. 3b and 4b that the regions between the respective thick and thin lines are unstable, noting that the unstable inner solution is not shown due to the fact that numerical integration does not converge on definitionally unstable solutions. The unstable regions in Figs. 3c and 4c are approximately around $\Omega = 3.23$ to 3.27 with slight variations for the different values of h_2, and these can only be seen clearly if the diagrams are enlarged.

A closer look at the first mode and the third order superharmonic is highlighted in Figs. 3b,4b and 3c,4c, respectively. Correlating with previous results it is seen that there is a consistent phenomenon, whereby as the softening cubic coefficient is increased, both the responses in the first mode of x_1 and x_2 show accentuated softening (see Figs. 3b and 4b). The amplitudes of both a_2

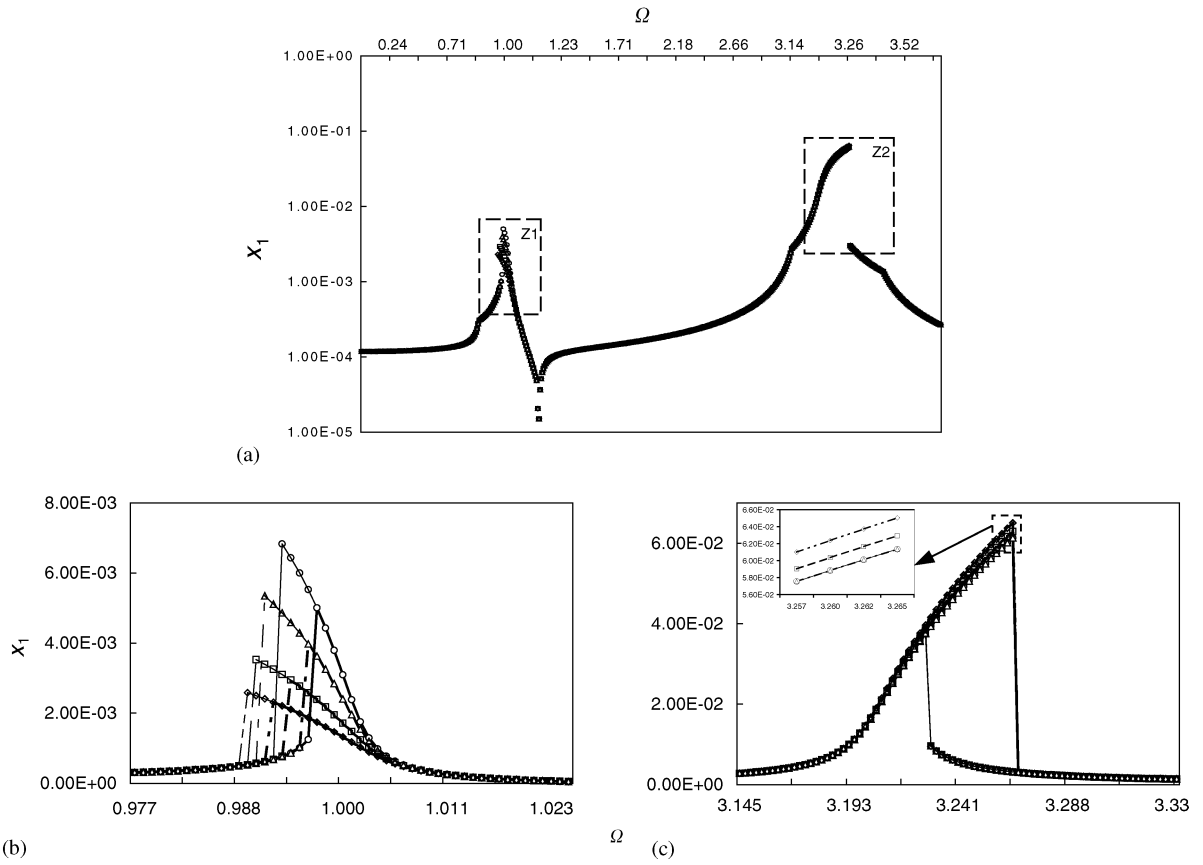

Fig. 3. (a) Direct numerical integration of non-dimensionalised x_1 versus Ω; (b) enlarged view of region Z1; (c) enlarged view of region Z2. Keys as for Fig. 2.

and x_2 are also marginally higher than a_1 and x_1. The results for the superharmonic in Figs. 3c and 4c cannot be compared to the analysis from the method of multiple scales because the latter only gives results for the first mode around the region close to the external resonance condition where $\varepsilon v = 0$, as in Eq. (19). However, it is interesting to note that when the softening cubic stiffness coefficient is increased, the characteristic shows a tendency to become more linear in Fig. 3c, whilst a more progressive hardening effect is visible in Fig. 4c.

3.3. Response bifurcations

Understanding the dynamics within Eqs. (1) and (2) can be extended by recourse to further numerical investigations. Using proprietary numerical analysis software, *Dynamics* 2 originated by Nusse and Yorke [33], bifurcatory behaviour of amplitude response x_1 as a function of the excitation frequency Ω, is depicted in Fig. 5. Again plotting with the same conditions as Sections 3.1 and 3.2, it is evident that for the third order superharmonic, as the cubic softening coefficient is increased from Figs. 5a–d, the response becomes more linear, hence correlating with Fig. 3c. The first mode is enlarged by a sweep up (see Figs. 5e–h) and a sweep down (see Figs. 5i–l) around the

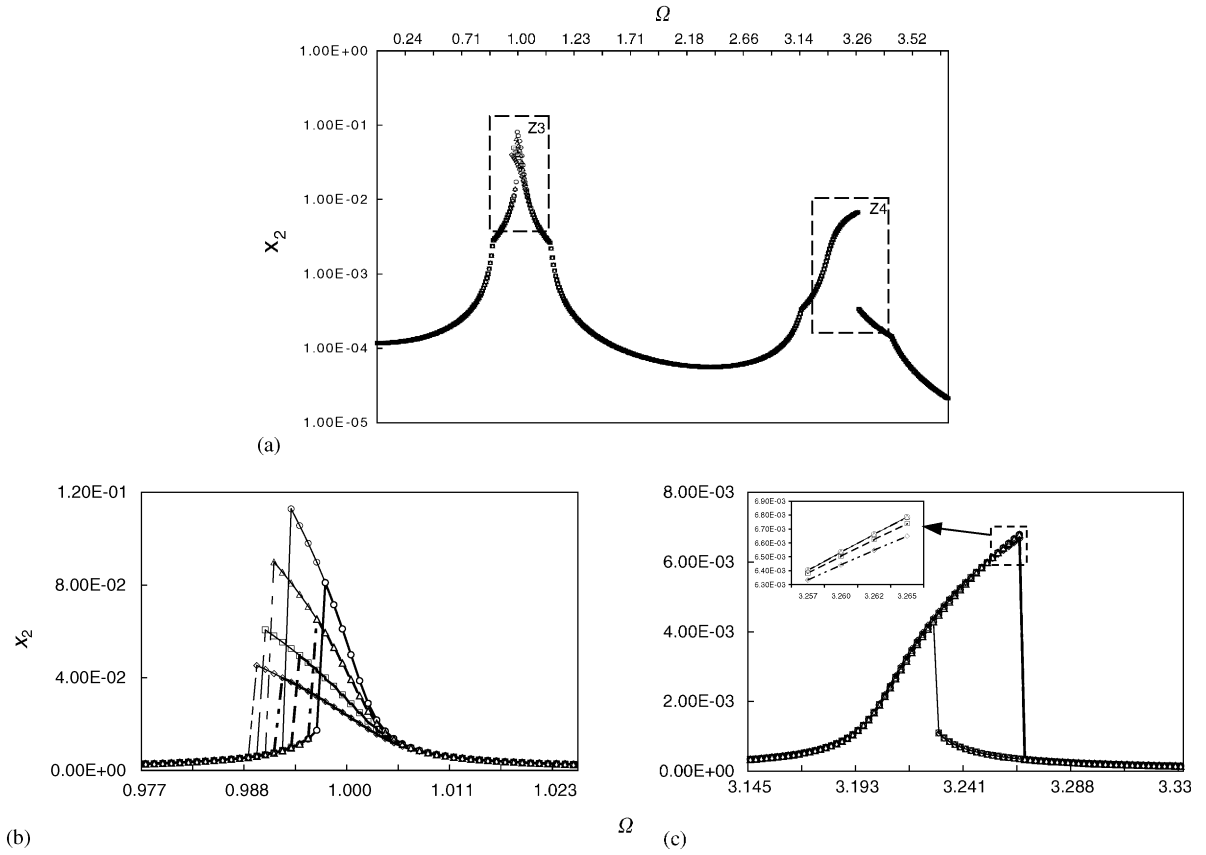

Fig. 4. (a) Direct numerical integration of non-dimensionalised x_2 versus Ω; (b) enlarged view of region Z3; (c) enlarged view of region Z4. Keys as for Fig. 2.

resonant region, and it is again evident that the cubic softening coefficient accentuates the softening effect, mirroring that in Fig. 3b.

Fig. 6 shows the bifurcation diagrams of amplitude response x_2 as a function of the excitation frequency Ω. Further evidence of accentuated softening by the increase of the cubic softening coefficient is extended in Figs. 6e–l. In the superharmonics of Figs. 6a–d, the increase of the cubic softening coefficient correlates with the numerical integration of Fig. 4c, whereby it becomes progressively more hardening. However, the graphs from *Dynamics 2* depict these as negative values, and the analysis is automatically truncated in Figs. 6c and d due to the computational limitations of the program. Despite these differences, both methods still show the same trend regarding the non-linear behaviour of the response curves. Given that necessary and sufficient conditions exists for possible chaos in the form of one stable and one unstable equilibrium then it appears that the presence of chaos in the downward sweep, but not in the upward sweep, is strongly influenced by the effect of the relevant initial conditions. This observation is made in the sense of Pezeshki and Dowell's [34] proposal that such Duffing systems manifest disconnections in the fractal form of the map of initial conditions and that this leads to chaos, or not, dependent on the precise nature of those initial conditions.

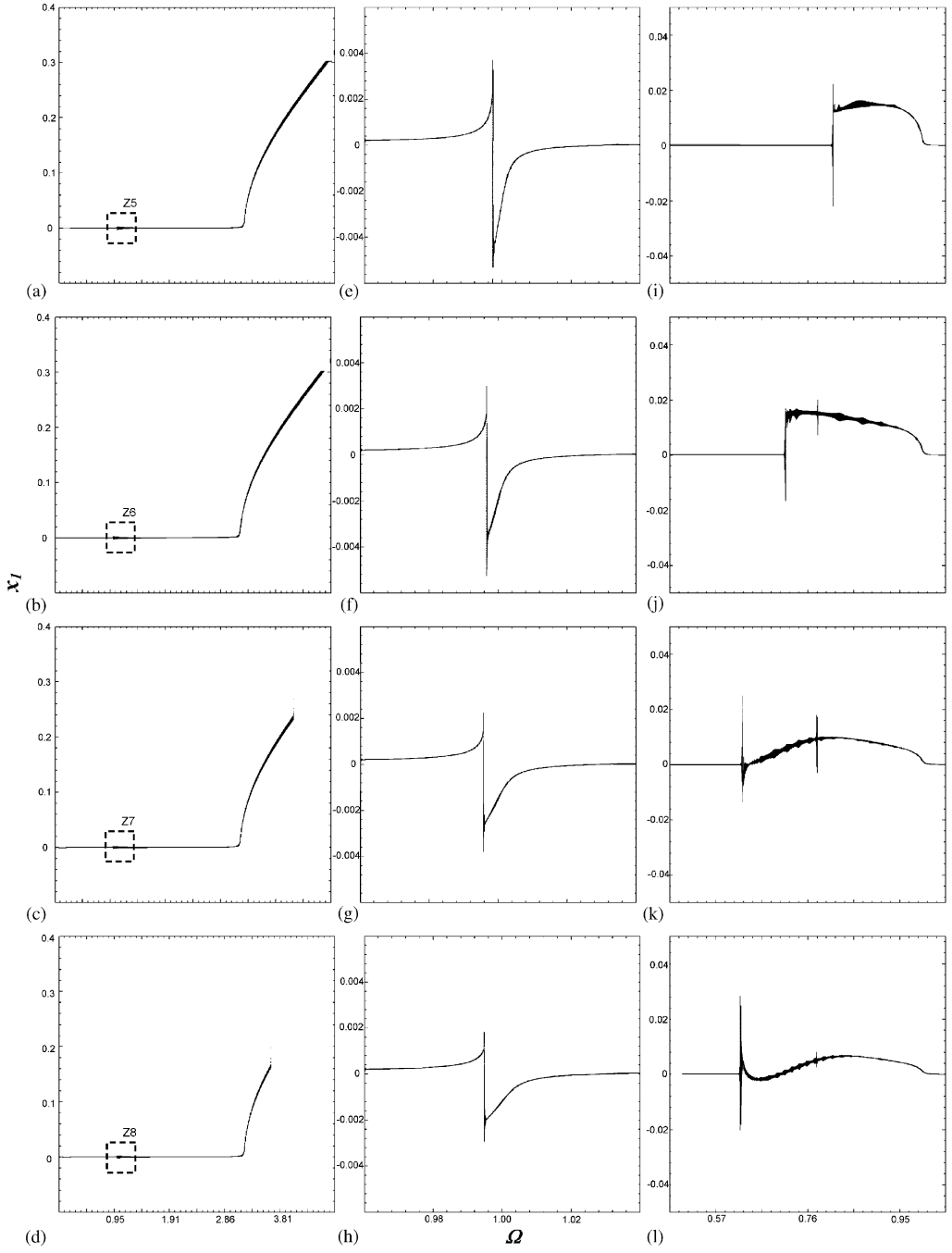

Fig. 5. Bifurcation diagrams showing non-dimensionalised x_1 as a function of Ω: (a) $h_2 = 0.008\,h_1$ for sweep-up analysis; (b) $h_2 = 0.0167\,h_1$ for sweep-up analysis; (c) $h_2 = 0.042\,h_1$ for sweep-up analysis; (d) $h_2 = 0.083\,h_1$ for sweep-up analysis; (e) is the sweep-up and (i) the sweep-down enlargement of region Z5; (f) is the sweep-up and (j) the sweep-down enlargement of region Z6; (g) is the sweep-up and (k) the sweep down enlargement of region Z7 and (h) is the sweep-up and (l) the sweep-down enlargement of region Z8.

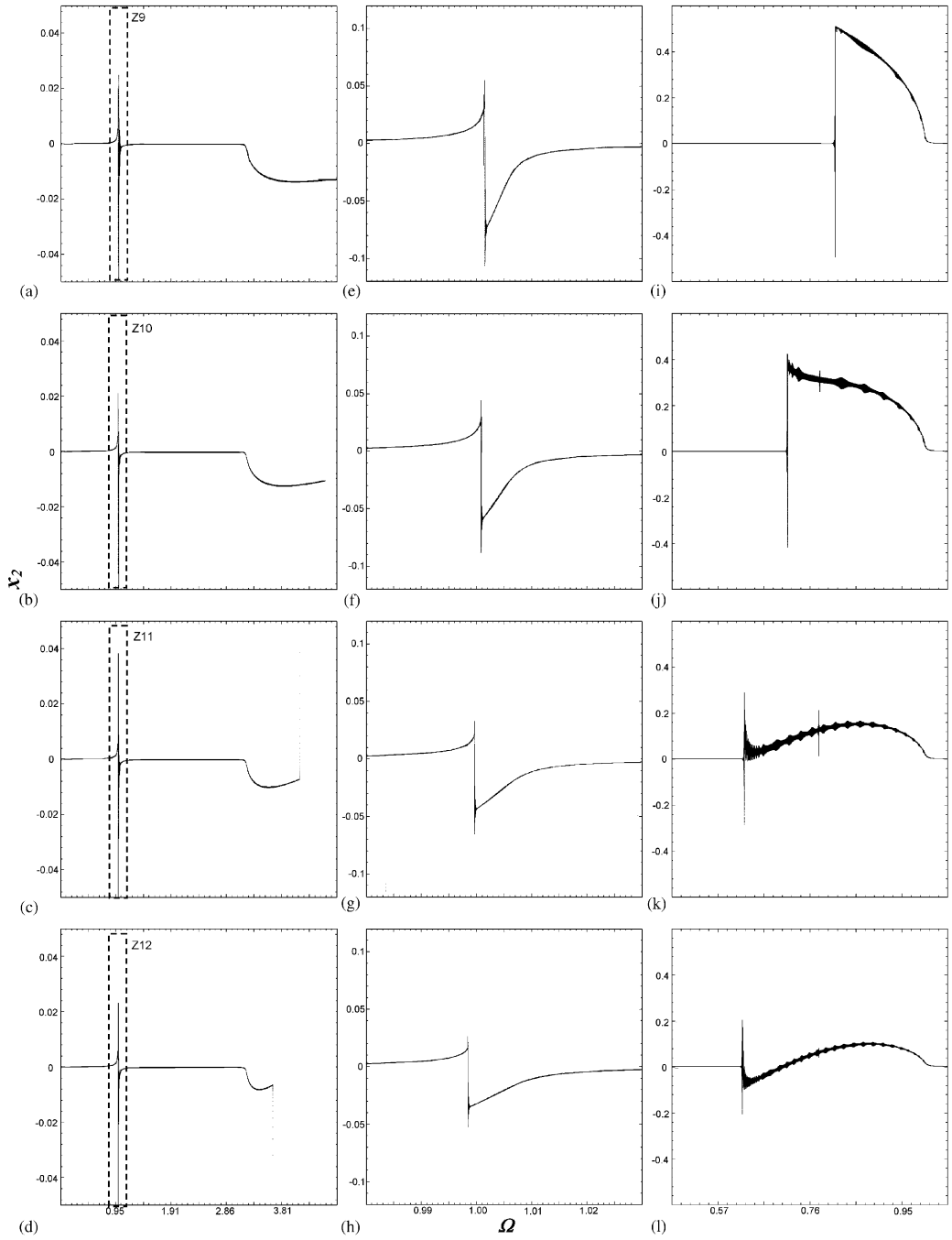

Fig. 6. Bifurcation diagrams showing non-dimensionalised x_2 as a function of Ω: (a) $h_2 = 0.008\,h_1$ for sweep-up analysis; (b) $h_2 = 0.0167\,h_1$ for sweep-up analysis; (c) $h_2 = 0.042\,h_1$ for sweep-up analysis; (d) $h_2 = 0.083\,h_1$ for sweep-up analysis; (e) is the sweep-up and (i) the sweep-down enlargement of region Z9; (f) is the sweep-up and (j) the sweep-down enlargement of region Z10; (g) is the sweep-up and (k) the sweep down enlargement of region Z11 and (h) is the sweep-up and (l) the sweep-down enlargement of region Z12.

The Lyapunov exponents of a system are a set of invariant geometric measures which describe, in an intuitive way, the dynamical content of the system. In particular, they serve as a measure of how easy it is to perform prediction on the system. Lyapunov exponents quantify the average rate of convergence or divergence of nearby trajectories, in a global sense. A positive exponent implies divergence, a negative one convergence, and a zero exponent indicates the temporally continuous nature of a flow. Consequently a system with positive exponents has positive entropy, in that trajectories that are initially close together move apart over time. The more positive the exponent, the faster they move apart. Similarly, for negative exponents, the trajectories move together. Thus, a positive Lyapunov exponent, is among the strongest indicators of chaotic motion.

Fig. 7 shows the Lyapunov exponents plotted for the bifurcations of the softening sweep down in Figs. 5i–l. In the regions of the softening characteristics, chaotic motions are evident by the positive values of the Lyapunov exponents. And as the cubic softening coefficient is increased, the system gets more softening and more chaotic, with a wider region of positive Lyapunov exponents.

Fig. 8 shows the bifurcation of the excitation acceleration when the excitation frequency is at its first mode eigenvalue of $\omega_{e1} = 209.828$ rad/s. By exaggerating the excitation acceleration to a high value, the periodic response for the smallest cubic softening coefficient in Fig. 8a (i.e., the most linear response in Sections. 3.1–3.3), bifurcates to what could be chaos as the coefficient is increased (see Figs. 8b–d). Also from these graphs, as the response appears to become chaotic, less excitation acceleration is required in each of the four cases, successively.

4. Experimental work

Ultrasonic systems behave in a noticeably non-linear fashion when run under certain conditions, particularly high power, continuously operating systems. The review paper on the non-linear dynamics of engineering components by Jerrelind and Stensson [35] gives a comprehensive definition of inherently non-linear behaviour in a wide range of practical components. In the food manufacturing industry, ultrasonic cutting is of considerable interest and this requires the application of high energy, ultrasonic oscillations within mechanical cutting tools over long operating periods. Because of this, the mechanical cutting tooling is required to be tuned so that modal energy does not leak out into audible lower frequency modes, both for reasons of efficiency, as well as longevity due to the minimisation of fatigue. Non-linear characteristics within the motion of the cutting tool are not particularly desirable because they can lead to multivalued responses, complex bifurcatory behaviour, unwanted inter-modal coupling, and also other phenomena such as combination resonances and very low cutting efficiency due to high levels of modal spill-over. For these reasons linearisation of the cutting tool response is seen as an important goal, however it has to be realised that non-linearity within the individual parts of the ultrasonic cutting system cannot necessarily be eradicated at source.

Because of this, the authors have proposed an alternative strategy in which the inherent and predominant non-linearities of the constituent parts of the ultrasonic cutting system are manipulated in such a way that their individual effects on the overall response can be effectively neutralised. In order to justify this work, a programme of experimental research was conducted in order to identify, and therefore confirm, the precise nature of the predominant non-linear

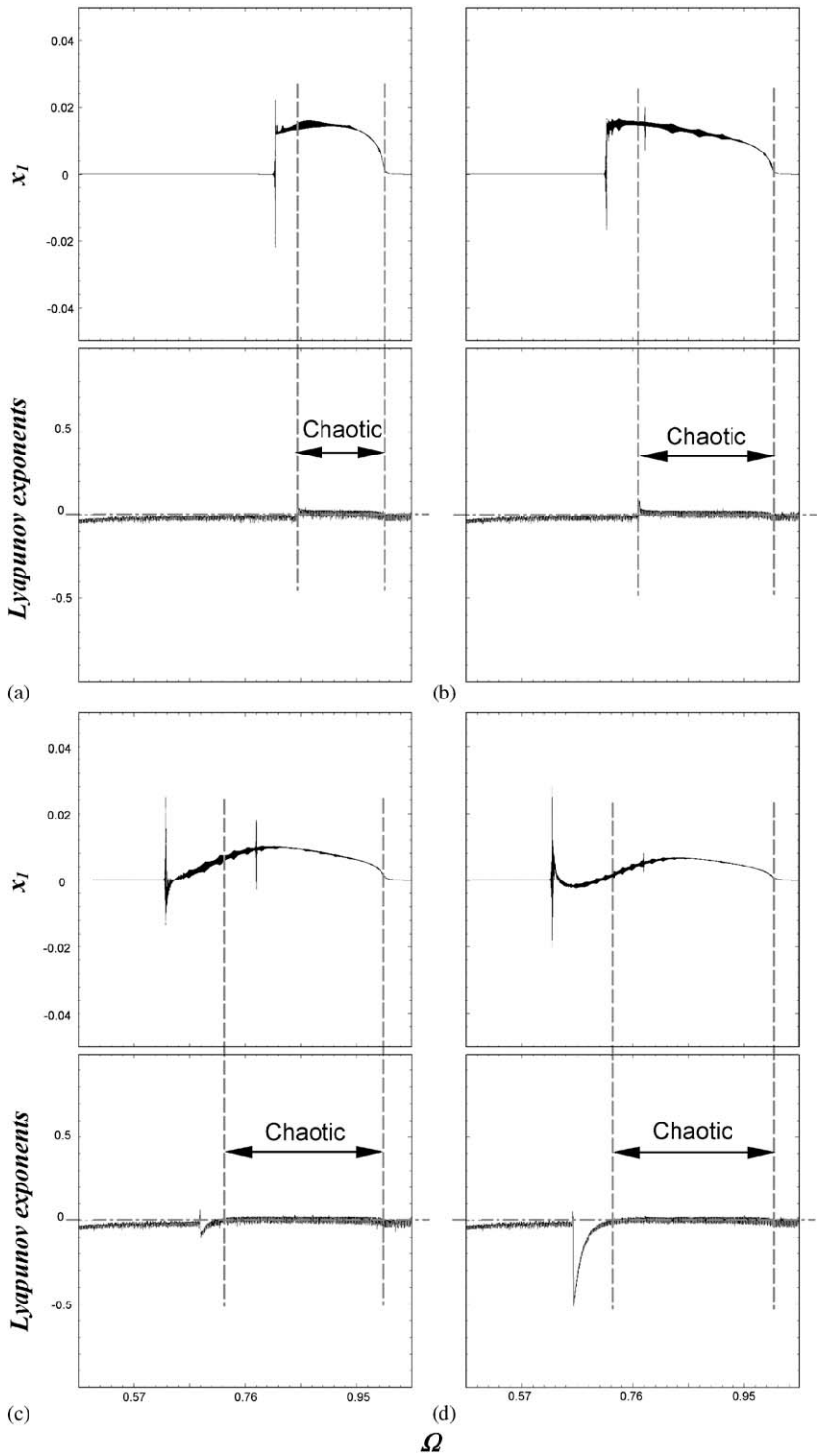

Fig. 7. Lyapunov exponents diagrams of non-dimensionalised x_1 (i.e., Figs. 5i–l): (a) $h_2 = 0.008\,h_1$; (b) $h_2 = 0.0167\,h_1$; (c) $h_2 = 0.042\,h_1$ and (d) $h_2 = 0.083\,h_1$.

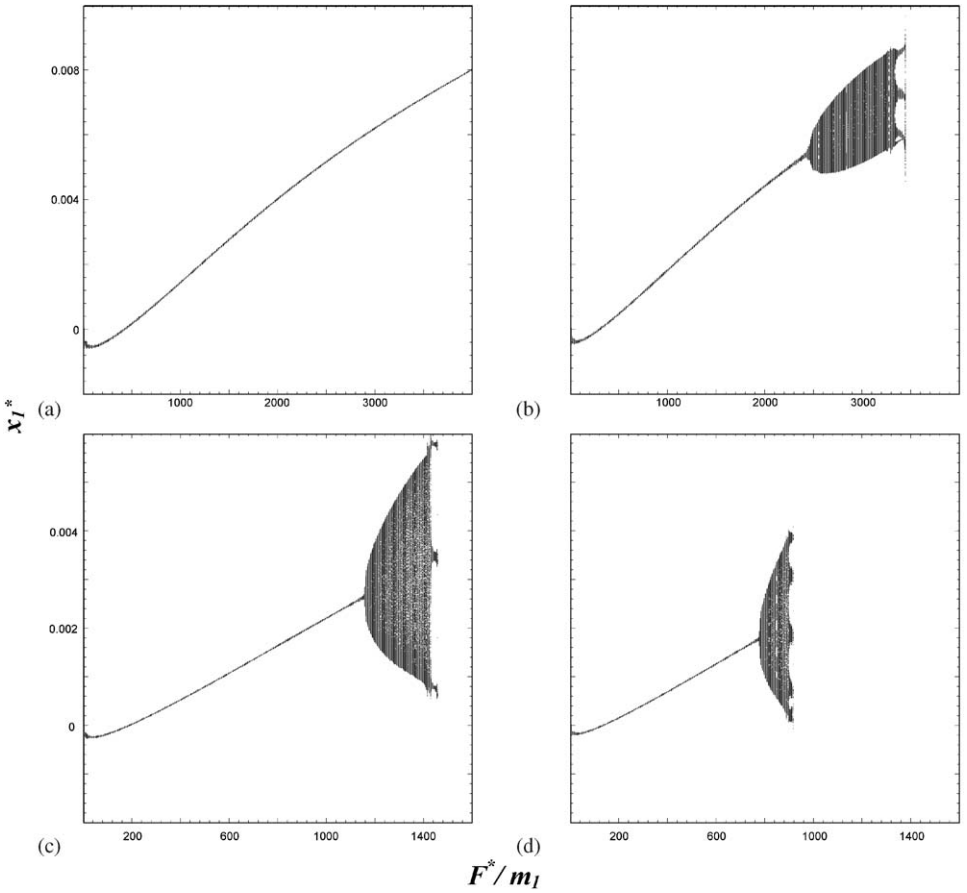

Fig. 8. Bifurcation of excitation force, $\Omega^* = \omega_{e1} = 209.828\,\text{rad/s}$ for (a) $h_2 = 0.008\,h_1$; (b) $h_2 = 0.0167\,h_1$; (c) $h_2 = 0.042\,h_1$ and (d) $h_2 = 0.083\,h_1$.

characteristics in each of the principal parts of an industrial ultrasonic cutting system. The findings of this work supported strongly the notion that such systems could be seen as two serially coupled sub-systems, each with opposing cubic stiffness non-linearities strongly predominating.

4.1. Instrumentation

Fig. 9 shows the experimental configuration for measuring the non-linear response of the ultrasonic system. The exciter (or *transducer*) is driven by a function generator connected to a signal amplifier. The vibration response of the transducer is then measured in the Cartesian x, y and z co-ordinates by means of a Polytek 3D Laser Doppler Vibrometer (3D LDV), allowing both in-plane and out-of-plane responses to be identified and monitored. A multi-channel data acquisition analyser connected to a portable computer enables the identification of system responses via contemporary signal processing software (DataPhysics SignalCalc 620).

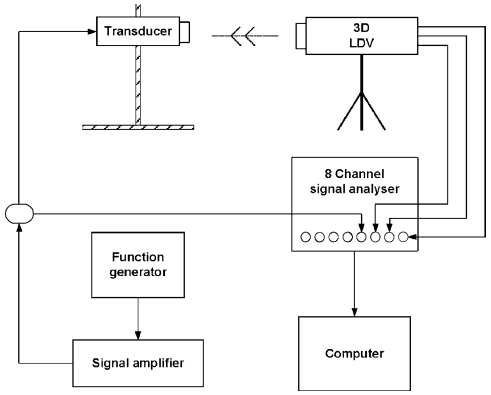

Fig. 9. Experimental set-up for response measurements.

(a)

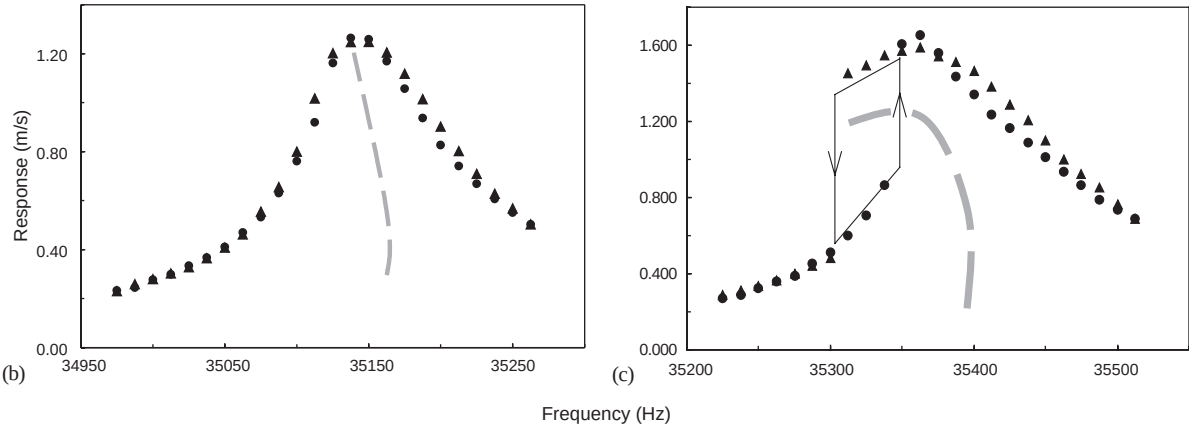

Fig. 10. Responses of an industrial ultrasonic transducer for two different excitation levels: (a) 35 kHz ultrasonic transducer; (b) transducer response at 30 V (●, up; ▲, down); (c) transducer response at 50 V (●, up; ▲, down).

4.2. Experimental results

The non-linear response characteristics of a typical industry standard 35 kHz high power ultrasonic transducer, as shown in Fig. 10a, can be obtained from an upward and downward stepped-sine sweep about its tuned frequency. The measured longitudinal mode response of the transducer is shown in Figs. 10b and c for two different excitation levels. Fig. 10b shows the transducer's response at an excitation of 30 V. Then, as the excitation is increased to 50 V as in

Fig. 10c, a region of hysteresis, combined with amplitude jumps and stable and unstable multivalued responses, becomes evident. As the frequency is swept upwards, there is an upward jump at approximately 35.34 kHz. Likewise, as the frequency is swept downwards, there is a downward jump effect at approximately 35.31 kHz. Within this small region hysteretic behaviour is plainly evident. The extremely narrow frequency band over which this occurs is a function of the high Q of such systems and underlines the importance of very precise design so that these effects can be reduced in such a way that the output of the cutting system to which the transducer is attached is as efficient and robust as possible. The frequency shifts in Figs. 10b and c are considered to be due to the effects of damping and thermal phenomena over the time duration of the experiment.

Ultrasonic block and bar-horns are specially machined components used to transmit vibration from a transducer to a tool or some other specialised tuned component. In this work, a simple bar-horn of aluminium material comprising a solid cylindrical rod (of length 1.5 λ) is attached to the transducer via a threaded stud half-screwed into both components (see Fig. 11a). At the 30 V excitation level, it can be seen that the response in Fig. 11b has less of a softening characteristic compared with that of Fig. 10b. A similar observation applies to the 50 V excitation level, with the characteristic region in Fig. 11c now having reduced in influence. The results obtained for typical industrially relevent equipment suggests that the strongly softening nature of the transducer can only be mitigated to a certain extent by the addition of characteristically hardening bar or block horns, and therefore that truly linearised response at the output of the system is not easily achieved.

Fig. 12 compares the non-linear performance of the same transducer, but attached directly to a 0.5 λ and a λ cutting blade with both blades manufactured from tool steel. In the first case at 30 V excitation level (see Fig. 12b), an even softer response is obtained than that for the transducer by

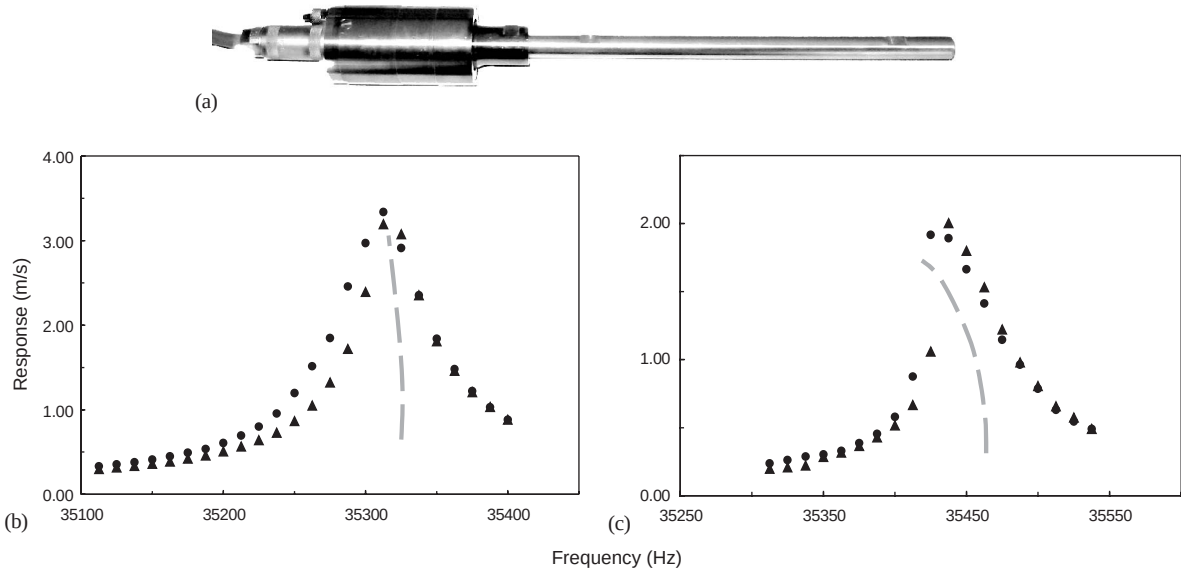

Fig. 11. Responses of an ultrasonic transducer and 1.5 λ bar-horn for two different excitation levels: (a) transducer with 1.5 λ bar-horn; (b) transducer and bar-horn response at 30 V (●, up; ▲, down); (c) transducer and bar-horn response at 50 V (●, up; ▲, down).

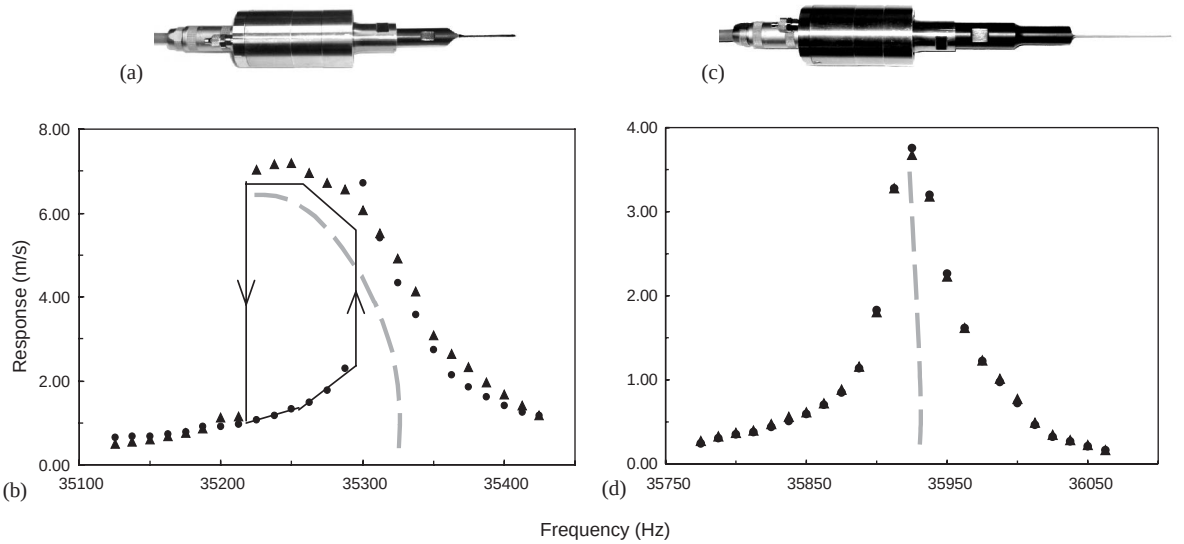

Fig. 12. Responses of an industrial ultrasonic transducer and 0.5 λ and λ blades for 30 V excitation level: (a) transducer with 0.5 λ blade and (b) its response (•, up; ▲, down); (c) transducer with λ blade and (d) its response (•, up; ▲, down).

itself. However, the λ blade exhibits a predominantly hardening characteristic and so the combined response is now significantly linearised as depicted in Fig. 12d.

4.3. Other influences on system non-linearity

These experimental investigations have also shown that the tightness of the screwed joints in between the coupled components contributes to the non-linear characteristics of the system. The joint between the transducer and the 1.5 λ bar-horn in Fig. 11a has been tightened with a higher torque and shows a more linearised response in Fig. 13a than that of a lower-torque joint in Fig. 13b.

The non-linear characteristics of the system can also be varied by means of the axial positioning of the stud within the joint. Fig. 14 shows three different configurations for the position of the threaded stud. It is evident that when the stud is fully fitted into the transducer-base (see Fig. 14a), the smallest non-linear region is evident in the system response at the blade tip compared with a configuration where it is half-fitted into the blade-base (see Fig. 14b). This effect is even more accentuated for the other extreme case where the stud is fully fitted into the blade-base (see Fig. 14c), for which the widest non-linear response region can be observed.

The theoretical analyses of Sections 2 and 3 investigate a simple discrete physical system which is a vehicle for the phenomena of interest but is not a direct model of the ultrasonic system discussed above. The resonance conditions predicted theoretically in those sections do not, therefore, explicitly define the resonant behaviour of the experimental system. However the theoretical model does indeed encapsulate the phenomena which can be observed, as discussed here, in the experimental system. For this purpose the superharmonic resonance condition is examined in Sections 2 and 3 because of the particularly clear-cut manifestation of the phenomena

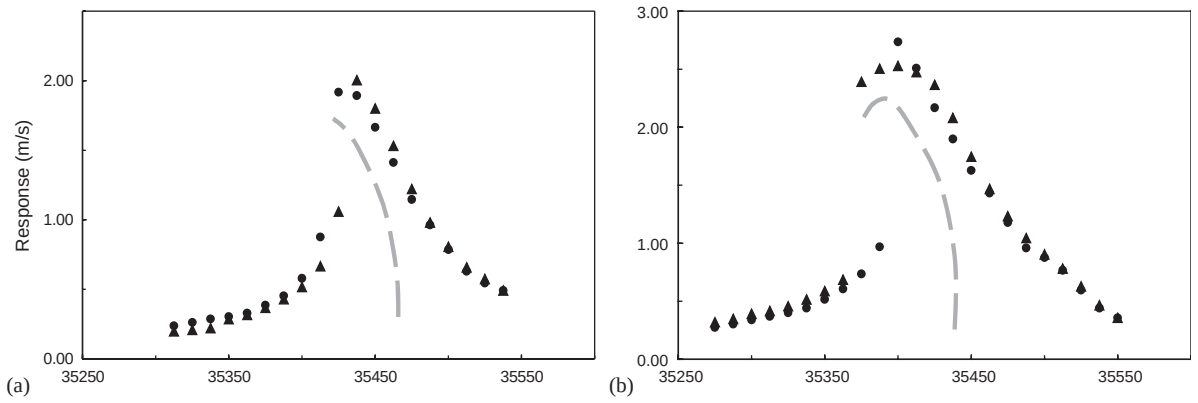

Fig. 13. Effects of joint tightness on the response for 50 V (●, up; ▲, down) excitation : (a) high torque and (b) low torque joint.

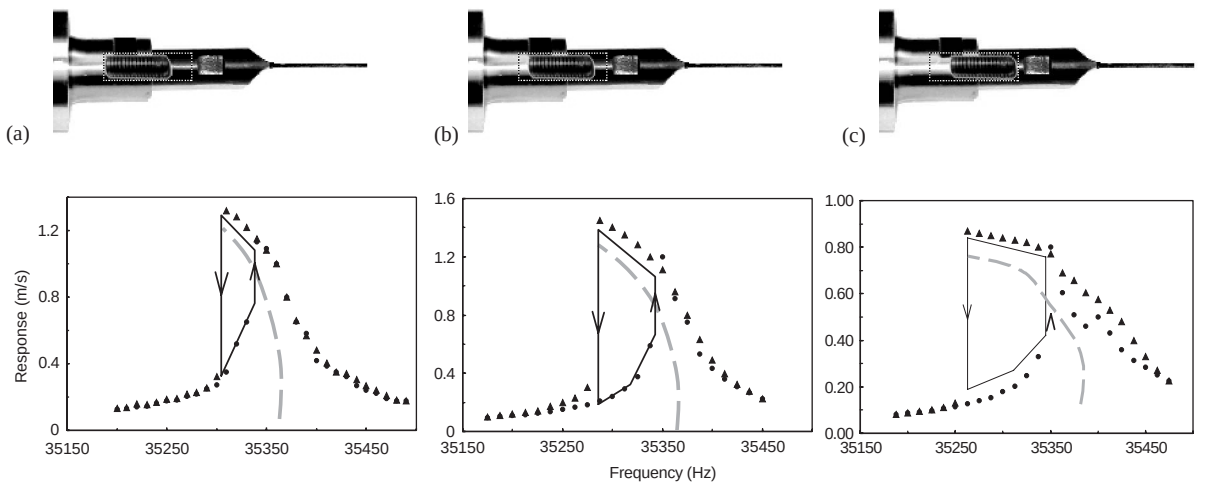

Fig. 14. Response of different stud configurations for 30 V (●, up; ▲, down) excitation: (a) stud fully fitted into transducer base; (b) stud half-fitted into blade base and (c) stud fully fitted into blade base.

of interest. These phenomena are also present in the subharmonic case and despite some algebraic complexities will also be present in the primary resonance case.

5. Conclusions

This paper has considered the issue of response modifications within an ultrasonic system as used within the food industry. The technique that has been developed is based on the exploitation of the natural mitigating effects of serially coupled non-linear sub-systems on the overall system response. It has been shown theoretically that certain non-linear effects can be advantageously

neutralised with the novel methodology of coupling another sub-system of opposite non-linear characteristic. It has been experimentally demonstrated that components with different geometries, materials and wavelengths are shown to possess different non-linear characteristic. By coupling them together, the overall non-linear response of the system has been usefully influenced.

The method of multiple scales and direct numerical method have both been used to solve for the superharmonic resonance of a two-degree-of-freedom Duffing-type system. Both analyses have shown good correlation regarding the behaviour of the responses when the softening cubic stiffness coefficient is varied. Further analyses on the dynamic bifurcations have also been carried out and similar behaviour when varying the softening cubic stiffness coefficient is evident.

Theoretically, by varying the softening cubic stiffness coefficient, this will have an effect on the overall linearity of the system. Applying this approach to an experimental ultrasonic system, a softening transducer can be somewhat linearised by adding another hardening component such as the 1.5λ bar-horn or the λ blade. However, adding another softening component such as the 0.5λ blade to the transducer makes the system even more softening in nature. Other ways of varying the linearity of the system can be achieved by the tightness of the joint and the axial positioning of the stud within the joint. A tighter joint and having the stud fully fitted into the transducer-base has been shown to give a more linear response.

This research provides some basic theory and understanding of how non-linear systems can be made more efficient. It has also initiated an identification of the non-linear characteristics of some ultrasonic components, and other factors that will influence the non-linearity. The practical goal has been to try to get the response of the blade (i.e., at the far end of the chain from the transducer) to be linear, irrespective of the fact that the transducer or the interconnecting components such as joints and bar-horn are all non-linear. This is tackled by means of exploiting the alternately non-linear characteristics of soft, hard, soft, hard, etc., effects that the serially linked transducer, joint, bar-horn, joint, and blade may provide.

Engineers and scientists are encouraged to use this new approach with prior understanding of the non-linearity of the particular components to be coupled. More research could stem from here in understanding how different variables (e.g., geometries, materials, wavelengths, etc.) will contribute to a component's non-linear characteristics. By obtaining a good basic understanding of each individual component, an ideal and robust overall linear system can ultimately be configured, and hence more reliable and efficient industrial systems can be designed. From here, one could intend to move onto fully representative *actual models of the ultrasonic system as initiated* from thinking about this simplistic theoretical vehicle, now that the experiments have borne out the theoretical proposal that this approach to the control of non-linear behaviour of such a system is possible.

Acknowledgements

The authors gratefully acknowledge the support of the Engineering and Physical Sciences Research Council (EPSRC) under grant GR/M58214/01 and Nestlé UK. They also wish to thank the anonymous reviewers for their insightful comments on the manuscript.

References

[1] M.P. Cartmell, J. Lawson, Performance enchancement of an autoparametric vibration absorber by means of computer control, *Journal of Sound and Vibration* 177 (2) (1994) 173–195 (doi:10.1006/jsvi.1994.1426).

[2] P. Woafo, H.B. Fotsin, J.C. Chedjou, Dynamics of two nonlinearly coupled oscillators, *Physica Scripta* 57 (1998) 195–200.

[3] A.H. Nayfeh, N.E. Sanchez, Bifurcations in a forced softening duffing oscillator, *International Journal of Non-Linear Mechanics* 24 (6) (1989) 483–497 (doi:10.1016/0020-7462(89)90014-0).

[4] J.A. Harris, A. Stevenson, On the role of non-linearity in the dynamic behaviour of rubber components, *Rubber Chemistry and Technology* 59 (1986) 740–764.

[5] J.A. Harris, Dynamic Testing under non-sinusoidal conditions and the consequences of non-linearity on service performance, *Rubber Chemistry and Technology* 60 (1987) 870–887.

[6] A.K. Mallik, V. Kher, M. Puri, H. Hatwal, On the modelling of non-linear elastomeric vibration isolators, *Journal of Sound and Vibration* 219 (2) (1999) 239–253 (doi:10.1006/jsvi.1998.1883).

[7] A.D. Morozov, A complete qualitative investigation of Duffing's equation, *Differential Equations* 12 (1976) 164–174.

[8] Y. Ueda, Randomly transitional phenomena in the system governed by Duffing's equation, *Journal of Statistical Physics* 20 (2) (1979) 181–196.

[9] Y. Ueda, Steady motions exhibited by Duffing's equation: a picture book of regular and chaotic motions, in: P.J. Holmes (Ed.), *New Approaches to Nonlinear Problems in Dynamics*, SIAM, Philadelphia, 1980, pp. 311–322.

[10] M.S. Soliman, Non-linear vibrations of hardening systems: chaotic dynamics and unpredictable jumps to and from resonance, *Journal of Sound and Vibration* 207 (3) (1997) 383–392 (doi:10.1006/jsvi.1997.1095).

[11] A. Smith, A. Nurse, G. Graham, M. Lucas, Ultrasonic cutting—a fracture mechanics model, *Ultrasonics* 34 (1996) 197–203 (doi:10.1016/0041-624X(95)00078-H).

[12] M. Lucas, G. Graham, A.C. Smith, Enhanced vibration control of an ultrasonic cutting process, *Ultrasonics* 34 (1996) 205–211 (doi:10.1016/0041-624X(95)00079-I).

[13] G. Graham, J.N. Petzing, M. Lucas, Modal analysis of ultrasonic block horns by ESPI, *Ultrasonics* 37 (2) (1999) 149–157 (doi:10.1016/S0041-624X(98)00050-X).

[14] A. Cardoni, M. Lucas, Enhanced Vibration performance of ultrasonic block horns, *Ultrasonics* 40 (2002) 365–369 (doi:10.1016/S0041-624X(02)00123-3).

[15] N.C. Shekhar, H. Hatwal, A.K. Mallik, Response of non-linear dissipative shock isolators, *Journal of Sound and Vibration* 214 (4) (1998) 589–603 (doi:10.1006/jsvi.1997.1468).

[16] N.C. Shekhar, H. Hatwal, A.K. Mallik, Performance of non-linear isolators and absorbers to shock excitations, *Journal of Sound and Vibration* 227 (2) (1999) 293–307 (doi:10.1006/jsvi.1999.2346).

[17] B. Ravindra, A.K. Mallik, Chaotic response of a harmonically excited mass on an isolator with non-linear stiffness and damping characteristics, *Journal of Sound and Vibration* 182 (3) (1995) 345–353 (doi:10.1006/jsvi.1995.0203).

[18] E. Ott, C. Grebogi, J.A. Yorke, Controlling chaos, *Physical Review Letters* 64 (11) (1990) 1196–1199 (doi:10.1103/PhysRevLett.64.1196).

[19] W.L. Ditto, S.N. Rauseo, M.L. Spano, Experimental control of chaos, *Physical Review Letters* 65 (26) (1990) 3211–3214 (doi:10.1103/PhysRevLett.65.3211).

[20] K. Pyragas, A. Tamasevicius, Experimental control of chaos by delayed self-controlling feedback, *Physics Letters* A180 (1993) 99–102 (doi:10.1016/0375-9601(93)90501-P).

[21] B. Hubiger, R. Doemer, H. Heng, W. Marienssen, Approaching nonlinear dynamics by studying the motion of a pendulum, III: predictability and chaotic motion, *International Journal of Bifurcation and Chaos in Applied Sciences and Engineering* 4 (1994) 773–784.

[22] L. Maestrello, Active control of panel oscillation induced by accelerated boundary layer and sound, *American Institute of Aeronautics and Astronautics Journal* 35 (5) (1997) 796–801.

[23] V.V. Bolotin, A.A. Grishko, A.N. Kounadis, C. Gantes, J.B. Robert, Influence of initial conditions on the postcritical behavior of a nonlinear aeroelastic system, *Nonlinear Dynamics* 15 (1998) 63–81.

[24] P.L. Chow, L. Maestrello, Vibrational control of a non-linear elastic panel, *International Journal of Non-Linear Mechanics* 36 (2001) 709–718 (doi:10.1016/S0020-7462(00)00038-X).

[25] L. Maestrello, The influence of initial forcing on non-linear control, *Journal of Sound and Vibration* 239 (4) (2001) 873–883 (doi:10.1006/jsvi.2000.3222).
[26] N. Aurelle, D. Guyomar, C. Richard, P. Gonnard, L. Eyraud, Nonlinear behavior of an ultrasonic transducer, *Ultrasonics* 34 (1996) 187–191 (doi:10.1016/0041-624X(95)00077-G).
[27] K.R. Asfar, Effect of non-linearities in elastomeric material dampers on torsional vibration control, *International Journal of Non-Linear Mechanics* 27 (6) (1992) 947–954 (doi:10.1016/0020-7462(92)90047-B).
[28] A.H. Nayfeh, *Perturbation Methods*, Wiley-Interscience, New York, 1973.
[29] A.H. Nayfeh, D.T. Mook, *Nonlinear Oscillations*, Wiley-Interscience, New York, 1979.
[30] M.P. Cartmell, *Introduction to Linear, Parametric and Nonlinear Vibrations*, Chapman & Hall, London, 1990.
[31] J.A. Murdock, *Perturbations: Theory and Methods*, SIAM, Philadelphia, PA, 1999.
[32] S. Wolfram, *The Mathematica Book*, 3rd Edition, Wolfram Media and Cambridge University Press, Cambridge, 1996.
[33] H.E. Nusse, J.A. Yorke, *Dynamics: Numerical Explorations*, 2nd Edition, Springer, New York, 1998.
[34] C. Pezeshki, E.H. Dowell, On chaos and fractal behavior in a generalized Duffing's system, *Physica D* 32 (2) (1988) 194–209 (doi:10.1016/0167-2789(88)90051-6).
[35] J. Jerrelind, A. Stensson, Nonlinear dynamics of parts in engineering systems, *Chaos, Solitons and Fractals* 11 (15) (2000) 2413–2428 (doi:10.1016/S0960-0779(00)00016-3).